Damage Detection Response Characteristics of Open Circuit Resonant (SansEC) Sensors

Kenneth L. Dudley, George N. Szatkowski, Laura J. Smith, Sandra V. Koppen, Jay J. Ely, Truong X. Nguyen
NASA Langley Research Center
Hampton, VA 23681 U.S.A.
Kenneth.L.Dudley@nasa.gov

Chuantong Wang and Larry A. Ticatch
National Institute of Aerospace
Hampton, VA 23681 U.S.A.

John J. Mielnik
Science and Technology Corporation
Hampton, VA 23681 U.S.A.

ABSTRACT

The capability to assess the current or future state of the health of an aircraft to improve safety, availability, and reliability while reducing maintenance costs has been a continuous goal for decades. Many companies, commercial entities, and academic institutions have become interested in Integrated Vehicle Health Management (IVHM) and a growing effort of research into "smart" vehicle sensing systems has emerged. Methods to detect damage to aircraft materials and structures have historically relied on visual inspection during pre-flight or post-flight operations by flight and ground crews. More quantitative non-destructive investigations with various instruments and sensors have traditionally been performed when the aircraft is out of operational service during major scheduled maintenance. Through the use of reliable sensors coupled with data monitoring, data mining, and data analysis techniques, the health state of a vehicle can be detected in-situ.

NASA Langley Research Center (LaRC) is developing a composite aircraft skin damage detection method and system based on open circuit SansEC (Sans Electric Connection) sensor technology. Composite materials are increasingly used in modern aircraft for reducing weight, improving fuel efficiency, and enhancing the overall design, performance, and manufacturability of airborne vehicles. Materials such as fiberglass reinforced composites (FRC) and carbon-fiber-reinforced polymers (CFRP) are being used to great advantage in airframes, wings, engine nacelles, turbine blades, fairings, fuselage structures, empennage structures, control surfaces and aircraft skins. SansEC sensor technology is a new technical framework for designing, powering, and interrogating sensors to detect various types of damage in composite materials. The source cause of the in-service damage (lightning strike, impact damage, material fatigue, etc.) to the aircraft composite is not relevant. The sensor will detect damage independent of the cause. Damage in composite material is generally associated with a localized change in material permittivity and/or conductivity. These changes are sensed using SansEC. The unique electrical signatures (amplitude, frequency, bandwidth, and phase) are used for damage detection and diagnosis. An operational system and method would incorporate a SansEC sensor array on select areas of the aircraft exterior surfaces to form a "Smart skin" sensing surface.

In this paper a new method and system for aircraft in-situ damage detection and diagnosis is presented. Experimental test results on seeded fault damage coupons and computational modeling simulation results are presented. NASA LaRC has demonstrated with individual sensors that SansEC sensors can be effectively used for in-situ composite damage detection of delamination, voids, fractures, and rips.

Keywords: Damage Detection, Composites, Integrated Vehicle Health Monitoring (IVHM), Aviation Safety, SansEC Sensors

ACRONYMS AND SYMBOLS

C	:	equivalent Capacitance
I_0	:	Current Amplitude
$\mathbf{J}(\mathbf{r})$	:	current density
l	:	trace length
L	:	equivalent Inductance
$\rho(\mathbf{r})$	:	charge density
$\varepsilon,$	:	free Space Permittivity
ε_r	:	relative Permittivity
μ_0	:	free Space Permeability
μ_r	:	relative permeability
ω	:	angular frequency

INTRODUCTION

The advantages of composite materials to the design, construction, and operation of modern aircraft have led to a revolution in the aerospace industry. The benefits of composites are found in weight reduction, superior strength, durability, and corrosion-free reliability over traditional metals. These benefits lead to reduced maintenance costs and lower necessity for in-service inspections. To fully leverage the advantages of composites in new aerospace vehicles and applications requires continuous investigation of novel technologies beyond the current state-of-the-art. [1][2]

The increased use of composites in aircraft structures means an increased potential for damage and/or failure of those composites. It can be difficult to predict the degree of composite damage or incipient faults while an aircraft is in use. This can be especially significant when the aircraft encounters a lightning environment. Statistics on lightning strikes indicates that in a typical year of operations a transport aircraft is likely to receive one or two lightning strikes. Depending on geographical regions, flight altitudes, routes, and traffic patterns, the frequency of strike occurrences can be higher than the average. Lightning strikes are a safety hazard to aircraft and can be especially so for those that have a considerable amount of composite material structures.[3] A means of in-situ health monitoring of composite materials for damage detection in real time would be highly desirable for enhancing aircraft safety.[4,5]

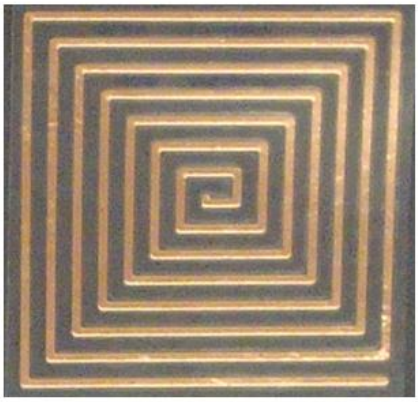

Fig. 1. A Generic Open-Circuit SansEC Sensor.

An open circuit resonant sensor has been developed for the purpose of in-situ detection and diagnostics of damage in non-conductive and conductive aerospace composite materials. The SansEC sensor is a planar resonant spiral or helix structure configured as an open circuit without (Sans) direct electrical connection (EC) to any recording instrumentation. It is composed of conductive material and formed in a manner such that the natural response of the geometry is to self-resonate when impinged upon by an external electro-magnetic field.

THEORY OF OPERATION

Electromagnetic resonance theory is well established for classical electromagnetic resonators such as resonant cavities, dielectric resonators, and LCR (inductive-capacitive-resistive) resonant circuits or structures. [6][7][8] The open-circuit resonator used as a sensor is a technology having unique features and applications. It is interrogated by a magnetic near field, self resonates at a specific fundamental frequency with useful harmonics, has a high power exchange efficiency, and responds to perturbations within its self-resonant field by detectable shifts in frequency, amplitude, phase, and resonance bandwidth.[9] This is the foundation for using open-circuit resonators for sensing purposes.

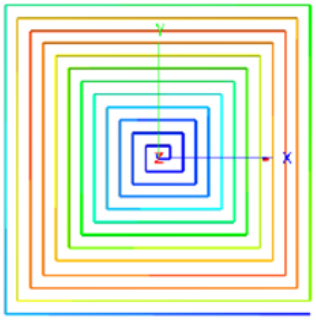

Fig. 2. Illustration of the Dominant Mode Current Distribution on an Open-Circuit Resonant Spiral (blue: lowest currents to red: highest currents)

The electro dynamic process of the open-circuit resonator is governed by Maxwell's equations with zero current boundary conditions at both ends of the resonant spiral. The free electrons carried by the conductor are uniformly distributed along the

conductive trace when no external source is applied, but when driven by an oscillating electromagnetic field the induced electromotive force (EMF) pushes the electrons carried by the conductor into the resonant state where the electrons move back and forth along the conductive trace. The time-dependent current profile along the conductive trace has the form:

$$I = I_0 cos(\frac{\pi x}{l}) e^{-i\omega t} \quad (1)$$

Where, $x \in [-l/2, l/2]$ is the parameterization coordinate along the length of the conductive trace; l is the trace length; I_0 is the maximum current amplitude; and ω is the angular frequency with t as time. The induced current along the conductive trace has a cosine distribution with the peak magnitude at the middle part of the trace and zero values at both ends of the trace. During each oscillation cycle, the total current will reach the peak magnitude twice (in opposite directions) and at these moments the energy stored in the resonator is in the form of the magnetic field.

From the continuity equation, the charge density profile has the following form:

$$q = q_0 sin(\frac{\pi x}{l}) e^{-i(\omega t + \frac{\pi}{2})} \quad (2)$$

Where, q_0 is the maximum charge density value. The charge is a sine distribution along the trace and creates the potential difference and consequently induces the electric field between the different localized segments of the trace. During each oscillation cycle, the electric field reaches its peak magnitude twice and at these moments the energy is stored in the electric field.

When resonating, the open-circuit sensor produces both electric and magnetic fields which occupy the space between the conductive traces and also penetrates into the space near the resonator. For the planar spiral sensor, the magnetic field and electric field will penetrate into the space beyond the planar surface of the sensor. This is an important feature for sensing purposes because it allows the sensor to measure the properties of the materials placed in close proximity.

Any physical quantity that affects the material's permittivity, permeability, or conductivity will affect the sensor's resonant parameters and therefore can be measured. Electric theory describes the LCR resonator by its lumped parameters of inductance L, capacitance C, and resistance R. For the self-resonant coil, the equivalent lumped parameters can be calculated based on the distributed parameters, as shown in equation (3) and equation (4), where μ_0 is the free space permeability, μ_r is the relative permeability, ε_0 is the free space permittivity, ε_r is the relative permittivity, and $\mathbf{J}(\mathbf{r})$ and $\rho(\mathbf{r})$ are the current and charge density functions along the conductive trace. [9]

$$L = \frac{\mu_0 \mu_r}{4\pi |I_0|^2} \iint \frac{\mathbf{J}(\mathbf{r}) \cdot \mathbf{J}(\mathbf{r}')}{|\mathbf{r} - \mathbf{r}'|} d\mathbf{r} d\mathbf{r}' \quad (3)$$

$$C^{-1} = \frac{1}{4\pi \varepsilon_0 \varepsilon_r |q_0|^2} \iint \frac{\boldsymbol{\rho}(\mathbf{r}) \cdot \boldsymbol{\rho}(\mathbf{r}')}{|\mathbf{r} - \mathbf{r}'|} d\mathbf{r} d\mathbf{r}' \quad (4)$$

However, the current and charge density functions are not measurable in actual experiments. Therefore, the equivalent inductance and capacitance values of a self-resonant coil are the calculated values and are used only for principle analysis. From equation (3) and equation (4), it can be clearly seen the dependency of inductance and capacitance upon the material's relative permeability μ_r and relative permittivity ε_r. If the material in the electric and magnetic field changes its permeability and/or permittivity, the resonator equivalent LC value will change correspondingly, so will the resonance parameters. It is notable that equation (3) and equation (4) are for the cases where the resonant sensor trace is totally embedded in the material having isotropic properties. For most actual applications, for example, the material is put on one side of the resonant sensor, the dependency function between the sensor parameters and the material properties is not obvious and needs to be characterized and calibrated by experiments or computational methods.

A NEW MULTI-FUNCTIONAL CONCEPT

Traditional methods for lightning protection for aircraft rely on a metal mesh or expanded metal foil embedded on or within the composite skin. This provides lightning protection and enhanced shielding effectiveness functions to the composite, but with no other benefit. [10] The SansEC sensor is a multifunctional new technology concept application for composite aircraft lightning strike protection, shielding effectiveness, and in-situ damage detection and diagnostics of aerospace composite structures. The concept is to apply an array of SansEC sensors, as shown in Fig. 3, to an aircraft surface forming a “Smart Skin” layer for the external composite covering. The SansEC sensor array includes a number of individual SansEC sensors and each individual SansEC sensor is an open-circuit conductive pattern sans (without) electrical connections.

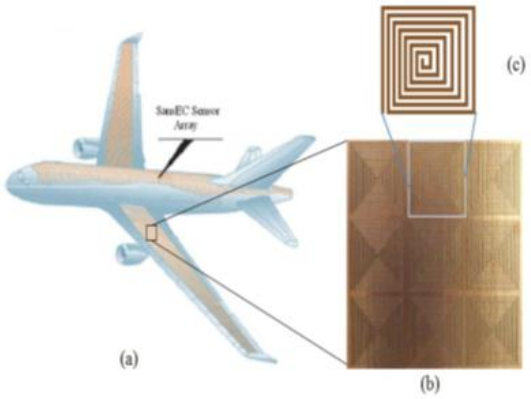

Fig. 3. Aircraft “Smart Skin” Concept using Surface Tiling Array of SansEC Sensors.

SansEC sensor is a wireless passive solution having each sensor in the array wirelessly powered and interrogated by an antenna through the magnetic near field. For interrogation of the sensor array on the aircraft surface, two methods can be used. The first method is for the in-situ measurement where the sensors are interrogated through antennas embedded with the sensor array. In this method, the sensor response is monitored by instrumentation computers in real-time during the flight. The interrogation system continuously scans the sensor array and compares the scanning result with the normal baseline stored in a database. An alarm will be given if serious damage is detected. The second method is for ground inspection and maintenance where the scanning of the sensor array is performed either by a robotic arm or a person using an external antenna. The second method is for the health check after lightning strike to detect any potential damage that cannot be visually discovered. The two interrogation methods are not exclusive to each other and the sensor system can use additional methods in different health check scenarios.

IN THE LABORATORY

With a promising new technology, a solid theory of operation, a new multifunctional sensor concept, and the desire within the Aviation Safety Program (AvSP) coupled with an interest by entities in Integrated Vehicle Health Management (IVHM) to assess the current and future health state of the composites in an aircraft, the High Intensity Radiated Fields (HIRF) laboratory at NASA Langley Research Center was tasked to establish an experimental capability for the investigation and development of applying SansEC sensors to the problem of lightning strike protection, enhanced shielding effectiveness, and damage detection and damage diagnosis of composite aerospace materials. The laboratory is used to develop SansEC test articles and conduct proof of concept experiments.

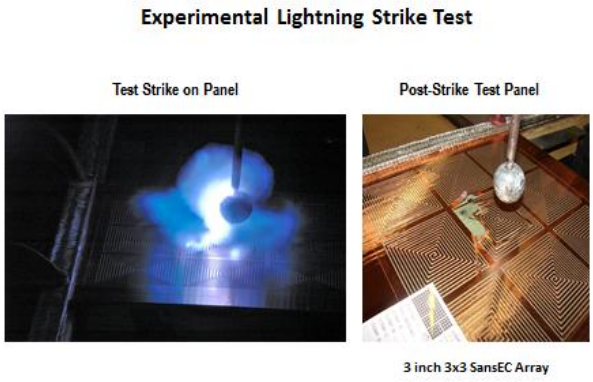

Fig. 4. Direct Effects Lightning Strike Test on a SansEC Array.

The laboratory is equipped with measurement instrumentation, tools, hardware, material resources, and various means of fabrication. Additional resources such as autoclaves and specialized equipment exist at the Research Center that can sometimes be leveraged for use.
The laboratory is capable of contracting to external facilities to conduct test such as direct effect lightning strike test seen in Figure 4 above.

The primary instruments used in experimental SansEC sensor research are network analyzers. The laboratory has three network analyzers that together cover frequency ranges from 10 kHz to 50 GHz. Figure 5 illustrates an Agilent E8364C Performance Network Analyzer (PNA) system interrogating a SansEC sensor. The PNA is a vector network analyzer capable of generating and measuring the frequency, magnitude, and phase of an electromagnetic wave. It is shown here connected to a near-field square loop antenna. [11] The loop antenna is used to illuminate or "ping" the SansEC sensor with a broadband frequency sweep from the network analyzer and then "listen" or receive the return response from the SansEC.

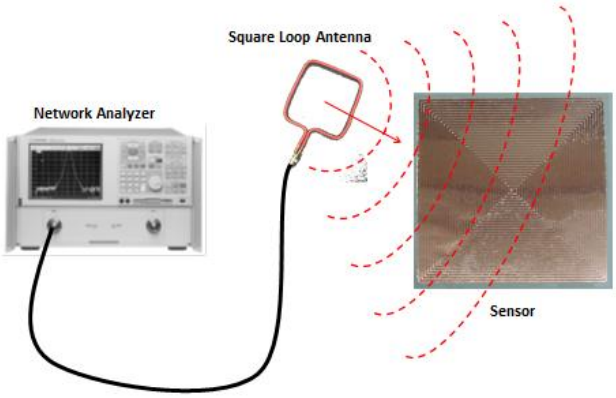

Fig. 5. RF Network Analyzer connected to Loop Antenna illuminating a SansEC Sensor.

The transmitted energy from the loop antenna excites resonant modes in the sensor. The resonant response frequency is usually comprised of a fundamental and associated harmonics related to the sensor geometry. The sensor is coupled to the loop antenna through the magnetic near field and the induced current (total current) in the sensor will have the maximum magnitude near its resonant frequency. At resonant state, the energy radiation of the sensor reaches its maximum value and so does the energy transferred to heat by the intrinsic resistance of the sensor trace. The resonant frequency of the sensor is indicated by the minimum amplitude of the reflection coefficient at the terminals of the loop antenna. The response is measured by the network analyzer as a return loss scattering parameter. The return loss S-parameter S_{11} is the reflection coefficient and is displayed on the network analyzer as a distinct amplitude resonance signature as a function of frequency.

Figure 6 is an example of an S-parameter plot and shows the resonance signature of a typical SansEC in Free Space and the same SansEC placed on the surface of an undamaged dielectric composite material. Note the 14 MHz frequency shift.

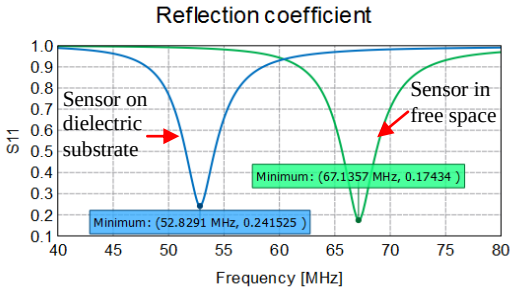

Fig. 6. S-Parameter plot depicting Resonances from two SansEC Sensor Experiments.

The initial laboratory experiments proved that a SansEC sensor placed on a material surface is capable of determining physical characteristics and qualities about the material upon which it is placed. [7][8][9][11] The detection of the differences in frequency and amplitude of the induced currents within a material substrate offers a means of detecting damage or changes to the state and condition of the material substrate.

COMPUTATIONAL EXPERIMENTS

Computational Electromagnetic Modeling (CEM) and simulation is a very useful research and development tool. By using iteration and feedback to model physical hardware and then validate the CEM against that physical hardware by means of experimental measurements, a better and more economical hardware product can be realized. Simultaneously a more robust design tool is developed that will enhance the next stage of design complexity. As understanding and confidence in the computational model and the experimental measurement increases, the ability to integrate sub-elements into larger systems occurs. In this manner we undertake steps in designing, integrating, and understanding SansEC resonant sensors both as computational models and physical hardware components. We use **FEKO**, "**FE**ldberechnung für **K**örper mit beliebiger **O**berfläche" or "Field Calculations for Bodies with Arbitrary Surface", a commercial computational electromagnetic software package to model our open-circuit resonant sensors. [12]

Response Characteristics of Internal Damage

A major challenge in composite damage detection is detecting the damage underneath a substrate surface. In general, the structural damage of the substrate is accompanied by a localized change of the material properties including permittivity, permeability, and conductivity in the damaged areas.

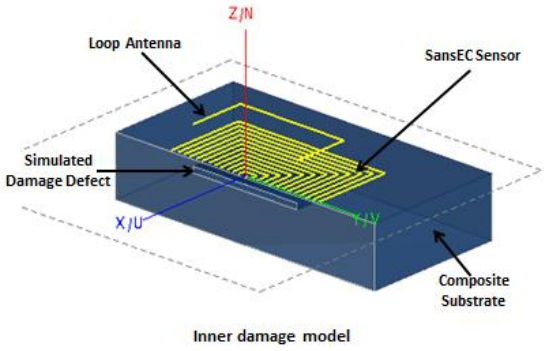

Fig. 7. Computational Model showing a 3D cross-section of a SansEC sensor on a Dielectric Composite with simulated internal Damage.

Figure 7 shows a 3D cross-section of a SansEC sensor on a dielectric composite model. The model is a Fiberglass Reinforced Polymer (FRP) composite substrate having inner structural damage simulating a defect. It is modeled by a free space slot. The slot has a size of 2.54 mm × 50.8 mm × 50.8 mm (0.1 inches × 2 inches × 2 inches) and is 2.54 mm (0.1 inches) from the substrate top surface. The localized permittivity change will change the effective permittivity of the substrate and consequently affect the resonant parameter of the sensor.

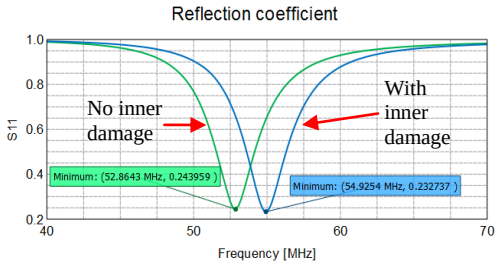

Fig. 8. S-Parameter plot depicting Resonances for substrates with and without Damage.

Looking at Figure 8, we see the reflection coefficient resonances of the sensor on the substrate with and without the inner damage slot. The resonant frequency of the sensor is shifted from 52.8643 MHz to 54.9254 MHz. The presence of damage in this case shifts the resonance signature by about 2 MHz. In measuring this frequency shift, the inner damage of the composite substrate can be effectively identified.

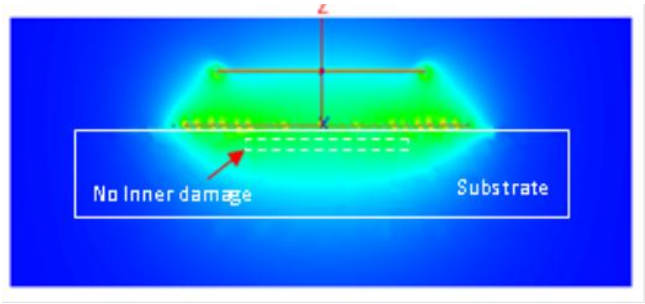

Fig. 9. Computational Model of the Electric Field Penetration from a SansEC sensor into a non-damaged Dielectric Composite

Figure 9 shows a cross-section of the electric field distributions of the sensor without the inner damage activated in the model. Figure 10 shows the electric field distributions of the sensor with the simulated inner damage activated.

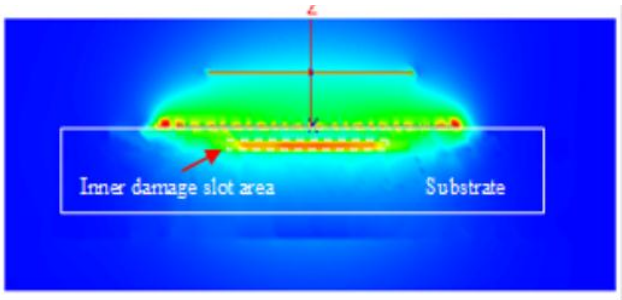

Fig. 10. Computational Model of the Electric Field Penetration from a SansEC sensor into a damaged Dielectric Composite.

The electric field has an obvious higher than normal density in the slot area. This is a great computational visualization that gives clear understanding of the electric field mechanism that allows the sensing of subsurface defects. This addresses realistic damages such as voids, delaminations, broken fibers, and heat damage in real composites. [13]

Response Characteristics of Surface Damage

Not only can SansEC sensors detect and identify delamination, punctures, cracks, and rips in composite materials, they are robust and damage tolerant. Since the SansEC sensor is typically on the surface of the composite substrate, the sensor will be the first line of protection during a lightning strike, hail impact, or any other type of external foreign object damage. [14][15][16] In the case where all of the sensor traces are damaged, the sensor will lose its resonant feature and has no response to the interrogator. However, when only a portion of the sensor trace is damaged, the remaining sensor traces form a new SansEC sensor shifting the operational resonance to a new frequency. Therefore, any damage of the sensor can be effectively detected by monitoring the sensor's resonant frequency. In actual situations, once the damaged sensor pattern is defined, a new baseline can be established. Figure 11 shows the model of a damaged sensor, which is one of many possible damage patterns. In this example, the sensor is damaged at one of its corners having four broken traces.

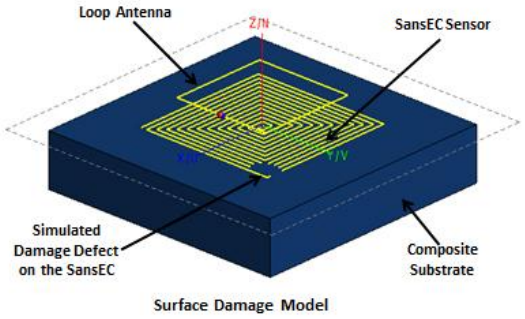

Fig. 11. Computational Model showing surface damaged SansEC sensor on a Dielectric Composite.

There is no single point on the sensor that if damaged will render the sensor non-functional. Each time the sensor is damaged, for example, by a puncture or partial split on the sensor body, it shifts the sensors self-resonant frequency to a new frequency range. This frequency shifting response is used as the signature in detecting structural damage of the sensor as well as damage within the composite substrate. The sensor response from the simulation result is shown in Fig. 12, where the resonant frequency shifted from 52.8571 MHz to 112.374 MHz. It can be seen that the sensor is very sensitive to the structural damage of the sensor trace. In general, even a small damage on the sensor body which breaks some of the sensor traces will have a significant shift on the resonant frequency. [13]

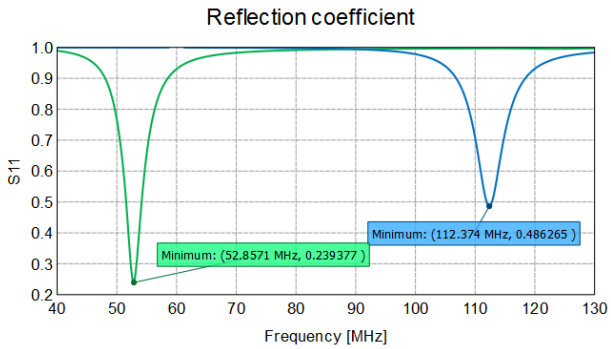

Fig. 12. S-Parameter plot depicting Resonances for a SansEC sensor with and without Damage.

Laboratory experiments and testing of various realistic aerospace SansEC test articles show good examples where the sensor traces are damaged yet the SansEC continues to function at a new baseline resonance frequency. These proof of concept experiments add validity to the computational models. In figure 13 we show a SansEC array test panel that has been struck by lightning. Three of the four SansEC sensors in the array showed some damage to the edge traces that comprised the individual sensors yet all four sensors continued to operate. The three damaged sensors shifted there self-resonance frequency to a new baseline.

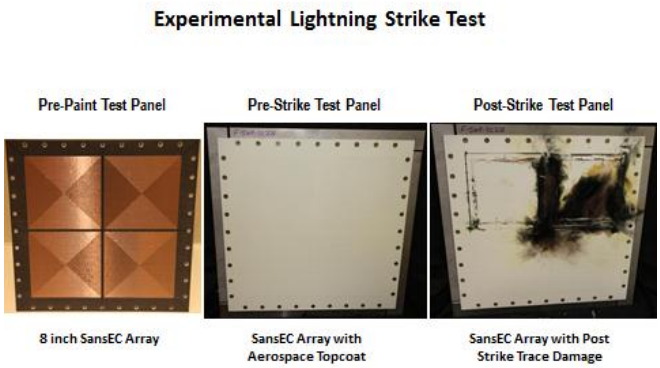

Fig. 13. Direct Effects Lightning Strike Test Panels depicting Pre and Post Strike Visuals

Response Characteristics of CFRP Damage

The composite materials for the experiments and computational models described thus far in this paper have all been non-conductive fiberglass reinforced polymers (FRP). These were modeled as ideal dielectric materials typical of aircraft FRP composite skin structures.

Other aerospace composite materials such as carbon fiber reinforced polymers (CFRP) are conductive. We developed a new CFRP model using the Surface Modeling Method in FEKO to simulate the complexity inherent in a realistic aerospace composite skin. The model is based on Hexcel carbon fiber test panels that were fabricated as composite panel test articles for lightning strike research. Based on these panels we also designed panels as physical test coupons that included known seeded faults. These experimental test panels were fabricated with a single top layer Hexcel Hexply 8552/A193-PW.3K-70-PW plain weave fabric as seen modeled in Figure 14 and five "clocked" or rotated layers of Hexcel Hexply 8552/AS4 unidirectional tapes shown modeled in Figure 15.

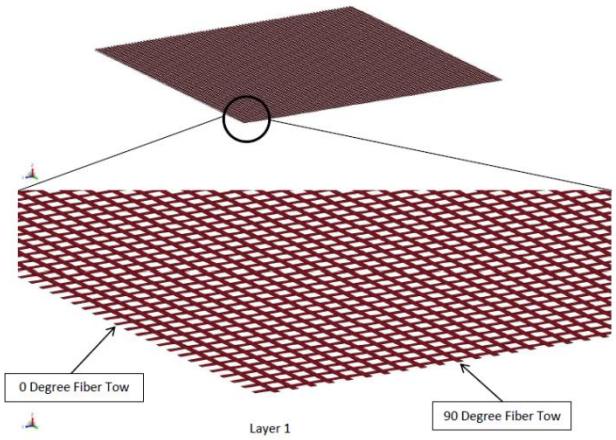

Fig. 14. CFRP Model Plain Weave Fabric Top Layer.

The top plain weave layer was modeled at the fiber tow level. The fiber tows were oriented at 0 degrees and 90 degrees. The next five layers in the stack consisted of the unidirectional tapes. They were oriented or "clocked" at +45 degrees, +90 degrees, -45 degrees, 0 degrees, and back to +45 degrees respectively. The ply thicknesses were nominally 0.15 mm (6 mils) thick.

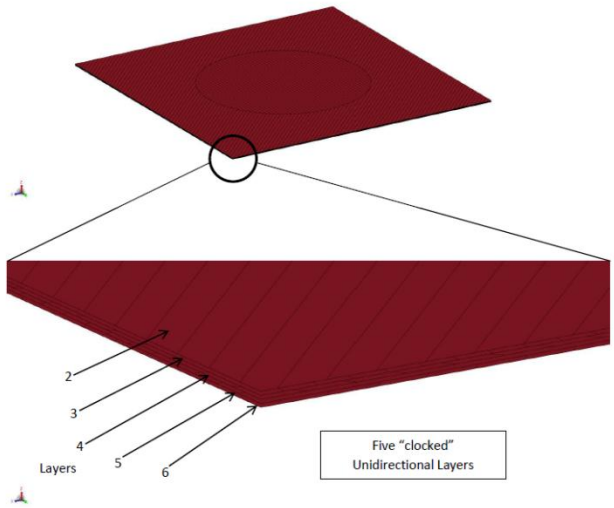

Fig. 15. CFRP Model Unidirectional Tape Stack Layers.

The CFRP model is much more complicated than the ideal dielectric FRP models. However, the model was implemented in a way to minimize the demand on computing resources for both meshing and solving. The geometry of the fiber tow in this model is parameterized such that control of the complexity of the model and the detailed micro-structure in the CFRP is realized. This enables the use of modest computing resources and the capability to attack complex problems and still converge to high fidelity solutions. With this, the stage was set to incorporate SansEC sensors onto the CFRP and implement referenced damage standards into the CFRP. [13][21]

Generally CFRP's are not as conductive as metals but are much more conductive than FRP's. When an oscillating electromagnetic field impinges upon a conductive material, the magnetic field can penetrate only a limited distance described by the "skin depth" effect. The skin depth of a material is defined as the depth below the surface of the conductor at which the current density has fallen to 1/e of the current at the surface. [13] A challenge with penetration into conductive composite materials is that the electromagnetic field is attenuated by the loss mechanism of the conductive substrate. When the composite substrate has high conductivity, the conductive surface of the substrate may absorb all of the electromagnetic field energy and render a SansEC sensor's resonance response non-detectable. For example, if a SansEC sensor made of copper is put on the surface of a highly conductive substrate, the sensor's response

characteristics will be totally lost. [22] To solve this problem, we developed a new method of using a thin dielectric material and a thin high magnetic permeability material between the sensor and the conductive substrate to control the field coupling. The dielectric material layer is used to insulate the conductive sensor trace from the conductive substrate. The high permeability material layer is used to concentrate the magnetic field inside the high permeability material. By partially covering the sensor area with high permeability material, a better impedance match to the conductive composite substrate can be established and the magnetic field can be effectively coupled into the composite. There are a number of ways to implement the geometry of the high permeability CFRP impedance matching cover and optimum methods are continuing to be explored.

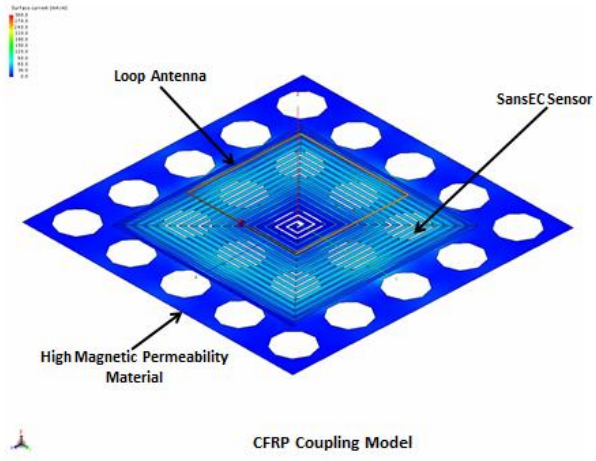

Fig. 16. SansEC CFRP Impedance Coupling Model.

For the illustration of the conductive coupling phenomena in this paper, a low frequency SansEC sensor is used. A perforated high permeability thin material layer is placed between the sensor and the conductive composite substrate and the area that is not covered by the high permeability material is covered by the thin dielectric layer. The SansEC configuration shown in Figure 16 was placed on top of the CFRP stack illustrated in Figures 14 and 15 and a series of computational electromagnetic modeling tests were conducted to test the permeation of electromagnetic signals into carbon fiber composites for the purpose of sensing and diagnosing damage. High fidelity computational electromagnetic models were run to simulate SansEC sensor operation on carbon fiber composites with common damage faults. The simulations were conducted on a baseline panel structure representative of a realistic aircraft skin, the same structure with seeded fault delaminations, and the same structure with a seeded machined core damage fault. The models and simulations were configured and run with damage faults of various sizes and at various ply depths. For the delaminations, the fabric or unidirectional tape ply separations were small 0.05 mm (2 mils), medium 0.5 mm (20 mils), and large 1.0 mm (40 mils). These delamination damages were simulated one ply depth beneath the top CFRP plain weave layer, three ply depths beneath the top layer, and five ply depths beneath the top. For the machined cores, two different sized cores where cut into various layers. A 37.5 mm core was removed from the unidirectional tape ply layer one depth beneath the top CFRP plain weave layer, three depths beneath, and five depths beneath. Likewise a larger 75 mm core was incorporated in the model in a similar fashion.[23][24]

Computational Electromagnetic CFRP Damage Model Test Matrix

Damage Type	Folder	Damage Model
No Damage	Baseline	Baseline
Delamination	Delamination 1	PlyDepth1 Damage 0.05mm
		PlyDepth1 Damage 0.5mm
		PlyDepth1 Damage 1.0mm
	Delamination 2	PlyDepth3 Damage 0.05mm
		PlyDepth3 Damage 0.5mm
		PlyDepth3 Damage 1.0mm
	Delamination 3	PlyDepth5 Damage 0.05mm
		PlyDepth5 Damage 0.5mm
		PlyDepth5 Damage 1.0mm
Machined Core	Core 37.5mm	PlyDepth1 Core 37.5mm
		PlyDepth3 Core 37.5mm
		PlyDepth5 Core 37.5mm
	Core 75mm	PlyDepth1 Core 75mm
		PlyDepth3 Core 75mm
		PlyDepth5 Core 75mm

Fig. 17. SansEC CFRP Damage Detection Computational Electromagnetic Model Test Matrix

The modeling effort enables an intuitive understanding of the electromagnetic field penetration interactions with carbon fiber composite damage. These insights were used to inform the experimental design and testing on actual seeded fault test panels.

In Figure 18 we see the cross sectional visualization of the electric field from a SansEC sensor on an un-damaged CFRP computational test panel. In Figure 19 we see the visualization of the electric field from the SansEC sensor on a panel with delamination damage underneath the CFRP top plain weave layer and between the first

CFRP unidirectional tape ply. In Figure 20 we observe the effects of the electric field from a SansEC sensor due to a puncture through the CFRP. The electric field bulging through the bottom of the test panel is very obvious. Finally in Figure 21 we see the cross sectional visualization of the electric field from the SansEC influenced by a void in the inter-ply layers of the carbon fiber test panel.

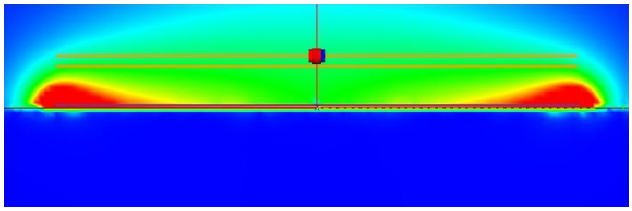

Fig. 18. Cross Section Electric Field Visualization of SansEC on CFRP with No Damage

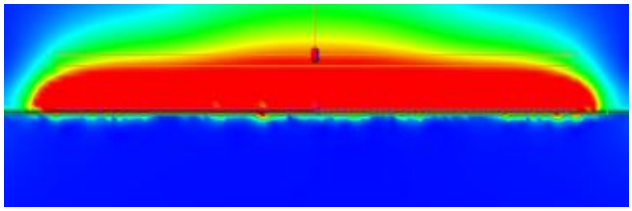

Fig. 19. Cross Section Electric Field Visualization of SansEC on CFRP with Delamination Damage

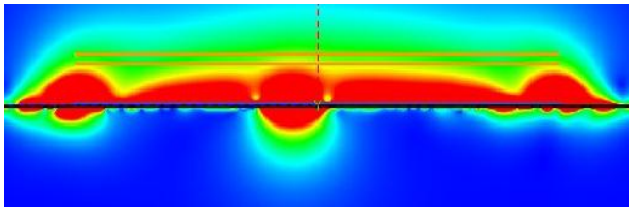

Fig. 20. Cross Section Electric Field Visualization of SansEC on CFRP with Puncture Damage

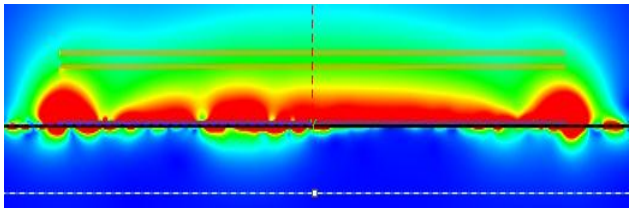

Fig. 21. Cross Section Electric Field Visualization of SansEC on CFRP with Void Damage

An experimental measurement based on the computational studies was conducted on the physical seeded fault test panel shown in Figure 22. These measurements demonstrate that a real SansEC sensor can detect delaminations in a real CFRP panel simulating an aircraft composite skin. The most remarkable demonstrations showed that the sensor could detect a 3 mil thick delamination down to the 5th ply of a carbon fiber composite with sufficient signal margins to indicate that the frequency resonance had shifted approximately 100 KHz between the baseline measurement (no delamination) and the measurement incorporating the delamination.[24][25]

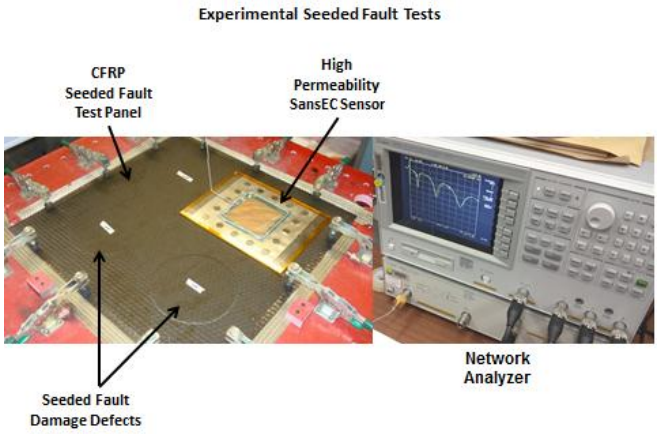

Fig. 22. Laboratory Test setup of the Seeded Fault Hexcel CFRP Delamination Test Panel

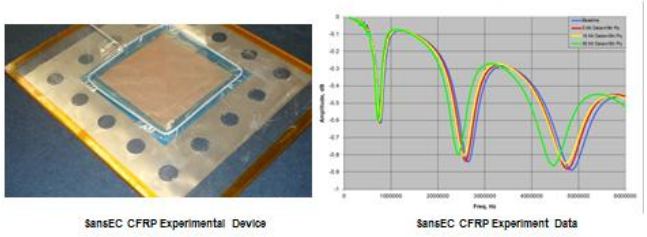

Fig. 23. High Permeability SansEC Sensor and Resonance Signature for Damage Detection

From the above results, it can be seen that the SansEC sensor with a high permeability material layer produced resonant responses, which confirmed that the high permeability material can be used on the conductive composite surface to reduce the effective attenuation and increase the sensor response amplitude. The experiment results of the SansEC sensor are shown in Figure 23, where the S_{11} S-parameter frequency plot presents the resonant response amplitude in dB

for the baseline measurement, and three seeded fault delamination conditions.

The feasibility is confirmed for using high permeability material to control the electromagnetic field coupling between the sensor and the composite substrate. The SansEC sensor coupled to a high permeability material can effectively reduce the attenuation effect on the electromagnetic field making it possible to measure changes in the physical value of permeability and permittivity within a conductive CFRP and thus detect and diagnose damage.

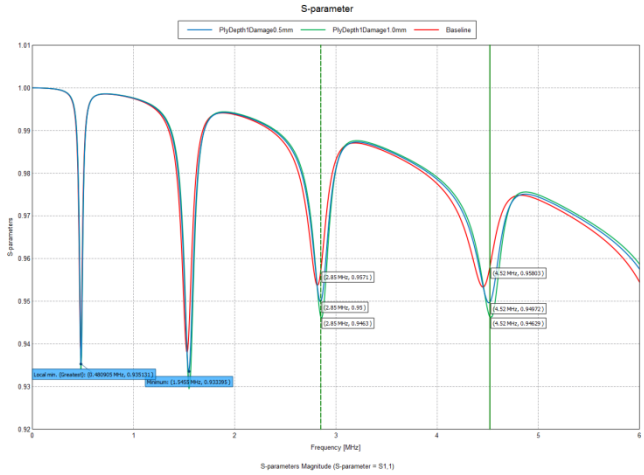

Fig. 24. CEM Data of SansEC Sensor Working on Conductive Composite using High Permeability Material

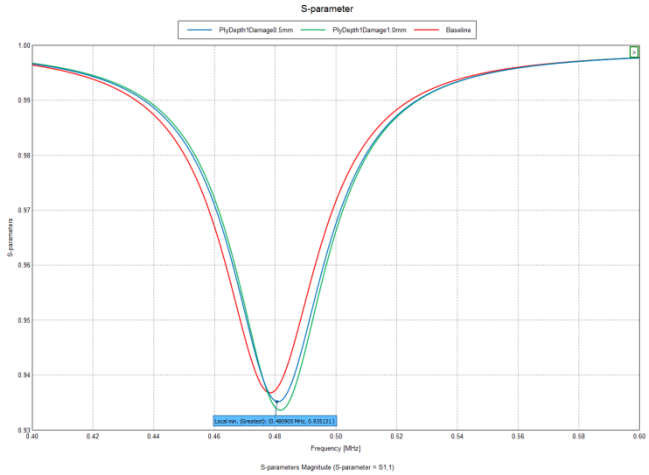

Fig. 25. Frequency Zoom-In on the first Resonance shown in Figure 24.

Even though the feasibility is confirmed, it is apparent from the experiment that more seeded fault test panels will be needed to thoroughly investigate the electrical characteristics of composite damage in order to achieve robust SansEC diagnostic capabilities.

The magnetic field coupling between the sensor and composite substrate is always a “trade-off” requiring optimized engineering design. For the sensing purpose in CFRP, it is needed for the strong electromagnetic field coupling to allow the field to penetrate deeply into the composite substrate. However, if the coupling is too strong, it will render the sensor’s response to be non-detectable. For keeping the sensor response and having good signal-to-noise ratio, the coupling ratio must be controlled to an acceptable limit. The strategy of using high permeability material covering the sensor with appropriate area percentage is an effective solution to this problem.

CONCLUSION

The SansEC sensor array used on the surface of composite structures is intended as a means for aircraft protection and as a means for damage detection and diagnostics. This provides many advantages over the traditional metal mesh method. The simulation results indicated that the sensor produced electromagnetic fields that penetrate into the space beyond the sensor surface. This allows the sensor to detect the inner damage of the composite substrate and detect any structural damage to the sensor trace. The ability of the open circuit resonant sensor to work after sustaining damage makes it especially suitable for aircraft lightning protection and damage detection. The sensor indicates damage to the composite by a frequency shift and higher electric field density in the damaged area, which lays the foundation for damage diagnosis. Experiments were conducted using the conductive composite substrate and the results confirmed the concept of using high permeability material to control the magnetic field coupling between the sensor and the composite. The coupling ratio can be controlled by the geometry of the sensor area covered by the high permeability material. This finding confirms the feasibility for damage detection and potential applications on realistic fiber glass composite and carbon composite aircraft structures. More detailed theoretical development, simulations, and physical experiments are considered for future study.

ACKNOWLEDGMENTS

The authors gratefully acknowledge NASA's Aviation Safety Program's Atmospheric Environmental Safety Technologies Project and the team members of NASA Langley Research Center's Fabrication Facility for fabrication of the seeded fault damage coupon. We acknowledge special appreciation to Dr. C.J. Reddy and Dr. Rensheng Sun at EM Software and Systems (EMSS) for useful discussions and technical support with advanced features in FEKO.

REFERENCES

[1] Long, M. W. and Narciso, J. D, "Probabilistic Design Methodology for Composite Aircraft Structure", DOT/FAA/AR-99/2 Report, No. ADA365683, 1999.

[2] Nobuo TAKEDA, Shu MINAKUCHI, Yoji OKABE, "Smart Composite Sandwich Structures for Future Aerospace Application -Damage Detection and Suppression-: a Review", Journal of Solid Mechanics and Materials Engineering, Vol. 1, No. 1, 2007, pp. 3-17.

[3] Franklin A. Fisher, J. Anderson Plumer, and Rodney A. Perala, Lightning Protection of Aircraft, 2nd ed., Lightning Technologies Inc., Pittsfield, 2004, Chapter 3.

[4] U. Polimeno M. Meo, "Detecting barely visible impact damage detection on aircraft composites structures", Composite Structures, Vol. 91, Issue 4, Dec 2009, Pages 398-402.

[5] John J. Mielnik, Jr., "Open Circuit Resonant Sensors for Composite Damage Detection and Diagnosis," NASA/CR-2011-216884, 2011

[6] Allen H. Meitzler, Ann Arbor, and George S. Saloka, Ford Motor Company, Dearborn, Mich, "Resonant Cavity Flexible Fuel Sensor and System," U.S. Patent No.5361035, Nov. 1, 1994.

[7] Ali Bitar, et al, Caterpillar Inc., Peoria, Ill, "Linear Position Sensor Using A Coaxial Resonant Cavity," U.S. Patent No.4737705, Apr. 12, 1988.

[8] Michael A. Fonseca, Mark G. Allen, Jason Kroh, and Jason White, "Flexible Wireless Passive Pressure Sensors for Biomedical Applications," Solid-State Sensors, Actuators, and Microsystems Workshop, Hilton Head Island, South Carolina, 2006, pp. 37-42.

[9] André Kurs, Aristeidis Karalis, Robert Moffatt, J. D. Joannopoulos, Peter Fisher, and Marin Soljačić, "Wireless Power Transfer via Strongly Coupled Magnetic Resonances," Science, Vol. 137, July 2007, pp. 83-86.

[10] Rowan O. Brick, Boeing Company, Seattle, Wash, "Lightning Protection System for Conductive composite Material," U.S. Patent No.4755904, July 05, 1988.

[11] Laura J. Smith, Kenneth L. Dudley, and George N. Szatkowski, "Computational Electromagnetic Modeling of SansEC Sensors," 27th International Review of Progress in Applied Computational Electromagnetics, Williamsburg, VA, Mar. 27-31, 2011.

[12] EMSS, "FEKO Comprehensive Electromagnetic Solutions User's Manual", EM Software & Systems-S.A. (Pty) Ltd. 32 Techno Avenue, Technopark, Stellenbosch, 7600, South Africa, 2011

[13] Chuantong Wang, Kenneth L. Dudley, and George N. Szatkowski EMSS, "Open Circuit Resonant (SansEC) Sensor for Composite Damage Detection and Diagnosis in Aircraft Lightning Environments", AIAA Paper 2012-2792, in Proceedings of the 4th AIAA Atmospheric and Space Environments Conference, 25-28 June 2012, New Orleans, LA

[14] Richard Minter, "Certification and continued airworthiness issues for composite structures," ICAS Biennial Workshop, Radisson Strand, Stockholm, Sweden, Sept. 5, 2011.

[15] Robert G. Thomson and Robert J. Hayduk, “An Analysis Evaluation of The Denting Of Airplane Surfaces By Hail,” NASA Technical Report No. TN D-5363, August, 1969.

[16] Thomas Boundreau, “CFR NPRM-Airworthiness Standards; Rain and Hail Ingestion Standards,” Federal Aviation Administration, Docket No. 28652, No. 96-12, Vol. 61, No. 155, August 9, 1996.

[17] Chuantong Wang, Woodard, S.E., and Taylor, B.D.; "Sensing of multiple unrelated tire parameters using electrically open circuit sensors having no electrical connections," IEEE Sensors Applications Symposium, New Orleans, 2009, pp.142-147.

[18] Stanley E. Woodard, Chuantong Wang, and Bryant D. Taylor, “Wireless temperature sensing using temperature-sensitive dielectrics within responding electric fields of open-circuit sensors having no electrical connections,” Measurement Science and Technology, Vol. 21, No. 7, July 2010.

[19] Stanley E. Woodard, "SansEC sensing technology — A new tool for designing space systems and components," Aerospace Conference, 2011 IEEE, Big Sky, 2011, pp.1-11.

[20] Stanley E. Woodard, "Functional Electrical Sensors as Single Component Electrically Open Circuits Having No Electrical Connections," IEEE Transactions on Instrumentation and Measurement, Vol.59, No.12, Dec. 2010, pp.3206-3213.

[21] Mohammadali Ansarizadehm, Alper Ozturk, and Robert Paknys, “Using FEKO for Electromagnetic Analysis of Carbon-Fiber Composite Structures,” 27th International Review of Progress in Applied Computational Electromagnetics, Williamsburg, VA, Mar. 27-31, 2011.

[22] Stanley E. Woodard and Bryant D. Taylor, “Magnetic Field Response Measurement Acquisition System,” NASA/TM-2005-213518, 2005.

[23] Dennis Roach, Larry Dorrell, Jeff Kollgaard, Tom Dreher, “Improving Aircraft Composite Inspections Using Optimized Reference Standards,” FAA Airworthiness Assurance NDI Validation Center / Sandia National Laboratories, 98AEMR-34, SAND-98-2022C, CONF-981115, 1998.

[24] Dave Galella, “FAA Inspection Research Activities for Composite Materials”, The 2006 Composite Damage Tolerance & Maintenance Workshop, July 20, 2006.

[25] Dennis Roach, “Improving In-Service Inspection of Composite Structures”, Sandia National Labs / FAA Airworthiness Assurance Center, 2008.